

# Laser surface remelting of powder metallurgy high-speed steel

J. IWASZKO\*

Czestochowa University of Technology, Department of Materials Engineering, ul. Armii Krajowej 19, 42-200 Czestochowa, Poland

**Abstract.** The effect of laser processing on the structure, microstructure and hardness of high-speed steel produced by powder metallurgy was investigated. The samples were surfaces remelted with impulse CO<sub>2</sub> laser radiation under different operation conditions. In the remelted layer, the presence of full remelting, partial remelting and heat affected zones was detected. As a result of concentrated laser beam treatment, microstructures characteristic of the rapid crystallization process were observed. The microstructure in the full remelting zone was characterized by a fine microdendritic structure with the average distance between the secondary axes of dendrites below 1 μm and the dissolution of primary carbides. Retained austenite was found in the remelted samples, the amounts of which depended on the treatment parameters and grew with an increase in the speed of the laser beam movement. There was no unequivocal effect of the distance of the irradiated surface from the focus of the beam focusing system on the content of retained austenite. Due to the presence of retained austenite in the remelted part, the hardness decreased by about 23% compared to the hardness of the material before the treatment. On the other hand, laser processing leads to strong refinement of the microstructure and eliminates the residual porosity of powder steels, which can increase the toughness and cutting performance of steel. The research also showed the possibility of shaping the geometry of the remelting zone by the appropriate selection of machining parameters.

**Key words:** laser remelting treatment, CO<sub>2</sub> laser, P/M high-speed steel, surface modification.

## 1. Introduction

High-speed steels (HSS) produced by powder metallurgy (P/M) are increasingly competing with steels produced in a traditional way. The advantage over their classic counterparts results from the more homogeneous microstructure, lack of segregation and banding of carbides as well as greater grain refinement [1, 2]. Compared with conventional cast or wrought parts, high-speed steel fabricated using powder metallurgy technology exhibits improved wear resistance, hardness, heat resistance and toughness [3]. The manufacturing of products by the powder metallurgy method is also characterized by a lower temperature of the manufacturing operation and more effective use of the starting material. All this makes steel made by powder metallurgy an unrivaled material in many aspects. However, the PM process is relatively complicated and generates high costs associated with powdering and hot isostatic pressing [4, 5]. The microstructure and properties of sintered high-speed steels are shaped primarily during the manufacturing process by optimizing individual technological operations and process parameters. The sintered steel microstructure can also be shaped by additional surface treatment which the material undergoes after or before the final heat treatment. One of the solutions increasingly used in shaping the microstructure of the surface layers of engineering materials is surface remelting carried out using concentrated heat sources [6–13]. The use of a laser beam, plasma arc or electric arc leads to the formation of a surface layer with completely new properties, which are the result of very fast melting of the material and rapid crystallization. In the case of the materials

produced by the powder metallurgy method, remelting carried out with concentrated heat sources also allows for the reduction of residual sintering porosity, whose presence results from the specificity of forming the material by the powder metallurgy method. Due to the residual porosity, some properties such as toughness, fatigue and wear resistance are often lower than those of the material processed by conventional routes [2]. The surface treatment of high-speed steels is most often carried out using laser technologies. The choice of laser technologies is dictated primarily by the ease of computer automation and control as well as the short process time. Laser surface melting does not involve change in the overall chemical compositions and no additional precious materials are required [13]. Also, it is worth noting that there is a possibility of precisely focusing the beam on a selected surface and achieving huge temperature gradients in the material, which affects the solidification rate of the melted material. Considering the nature of high-speed steels and the specificity of the effect of laser heat on the material being processed, the use of laser technology in modifying the surface of high-speed steel seems to be a promising solution [14]. As the literature data indicate, the attention of research teams focuses mainly on the surface remelting of high-speed steels produced in a conventional manner [14–20]. For instance, in paper [14] Chau et al. analyzed the effect of time and energy parameters of the pulsed laser treatment on the structure formation and hardness of the R6M5-type HSS upon surface melting after full heat treatment. They found that the laser-induced remelting causes a significant refinement of both the dendritic structure of the solid solution and of the carbide constituent of high-speed steel. As a result of surface remelting, the hardness of high-speed steel decreased. The hardness changed in a wide range and did not exceed the hardness of the heat-treated base material. In turn, J. Arias et al. [20] analyzed the microstructure of Nd:YAG continuous wave laser-melted surface of AISI M2 high-speed

\*e-mail: iwaszko@wip.pcz.pl

Manuscript submitted 2020-07-03, revised 2020-08-21, initially accepted for publication 2020-09-14, published in December 2020

steel. They found a dendritic structure in the melted zone and a heterogeneous cellular structure in the partially melted zone.  $M_2C$  carbides with different morphologies were identified in the resolidified surface layer after laser-melting. The surface layer obtained after laser-melting of the surface was homogeneous and highly refined, with no cracks, discontinuities, or porosity.

From the literature data it can be seen that there are decidedly fewer works on the surface remelting of steels produced by powder metallurgy [2, 21–26], including very few studies on high-speed steels [2, 23–26]. For example, the authors of [25] subjected two high-speed steels, ASP23 and ASP30 formed by powder metallurgy, to surface remelting. The machining was carried out using a 2.5-kW Nd:YAG laser. It was found that the laser-melted zone of the HSSs consisted of fine dendrites of austenite crossed by an extremely fine carbide precipitation network or the eutectic without primary large carbides and with high chemical homogeneity. Compared to the annealed and conventionally hardened HSS, the corrosion resistance of laser-melted HSS was found to be improved, as evidenced by a shift in the corrosion potentials in the noble direction and a reduction in the corrosion current densities by 5.5 times. In turn, Jurci et al. [21] subjected PM ledeburite steel Vanadis 6 to laser remelting. The surface treatment was carried out using an Nd:YAG laser with an irradiation wavelength of 1064 nm, operating in a continuous regime. The steel was subjected to standard heat treatment, i.e. quenching and tempering before surface remelting. They found that the microstructure consisted of the matrix and two morphological types of carbides, namely  $M_7C_3$  and MC types. The matrix was mostly austenitic, but the presence of a portion of martensitic needles was also evident. They also found that laser surface melting and subsequent rapid solidifying led to softening of the material, due to the presence of retained austenite.

Surface remelting of sintered high-speed steels is an issue with a high cognitive and application potential, which is unfortunately relatively poorly documented in the world literature. This fact prompted the author of this work to carry out his own research in this area. The assessment of the possibilities of using surface remelting in shaping the microstructure of sintered high-speed steels is the subject and the main aim of the research work.

## 2. Materials and experiment procedures

**2.1. Materials.** The test material consisted of cuboidal samples with dimensions of  $60 \times 30 \times 9$  mm made of commercial sintered high-speed steel, whose chemical composition is given in Table 1. The steel used in the work is intended for heavily loaded tools, both for machining and for plastic working. This steel is particularly recommended, e.g. for machining metals based on nickel and titanium, and for all types of tools that require very high compressive strength. Before laser melting, the specimens were subjected to standard heat treatment, i.e. quenching and then tempering three times (Table 2). The austenitization temperature was  $\approx 1180^\circ\text{C}$ . The treatment was carried out in a vacuum oven.

Table 1  
Chemical composition of P/M HSS

Content of elements [wt%]					
W	Co	V	Cr	Mo	C
10.14	7.75	4.73	4.64	1.87	1.66
Si	Mn	Ni	P	S	Fe
0.56	0.29	0.16	0.02	0.017	rest

Table 2  
Heat treatment process of P/M HSS

Heat treatment		Temperature/Time
Quenching	Heating I	$550^\circ\text{C}/900$ s
	Heating II	$850^\circ\text{C}/900$ s
	Austenitizing	$1180^\circ\text{C}/150$ s
Tempering		$3 \times 560^\circ\text{C}$ for 7200 s

**2.2. Laser processing.** Surface remelting treatment was performed using a  $\text{CO}_2$  laser with impulse work characteristics generating a laser beam of TEM<sub>00</sub> mode. No coatings were applied to enhance the absorption of laser radiation. The laser power was 1200 W, pulse duration 45 ms, and pulse interval 40 ms. The distance of the irradiated surface from the focus of the beam focusing system  $\Delta l$  was from 28 mm to 48 mm, and focal length  $f$  was 250 mm. Laser head speed  $V$  was 750 mm/min, 800 mm/min and 850 mm/min. The processing parameters as well as the bandwidth and depth of microstructural changes are presented in Table 3. The measurement of the microstruc-

Table 3  
Surface treatment parameters and dimensions of modified zone

No.	Laser head speed $V$ [mm/min]	Distance of irradiated surface from focus of beam focusing system $\Delta l$ [mm]	Bandwidth [mm]	Depth of microstructural changes [mm]
1	750	28	$3.20 \pm 0.1$	$4.81 \pm 0.1$
		32	$3.18 \pm 0.1$	$4.12 \pm 0.1$
		36	$1.66 \pm 0.1$	$1.07 \pm 0.05$
		40	$1.86 \pm 0.1$	$0.97 \pm 0.05$
		44	$2.08 \pm 0.1$	$0.93 \pm 0.05$
		48	$2.32 \pm 0.1$	$0.83 \pm 0.05$
2	800	28	$2.90 \pm 0.1$	$4.65 \pm 0.1$
		32	$2.96 \pm 0.1$	$3.84 \pm 0.1$
		36	$1.55 \pm 0.1$	$0.89 \pm 0.05$
		40	$1.71 \pm 0.1$	$0.87 \pm 0.05$
		44	$1.99 \pm 0.1$	$0.87 \pm 0.05$
		48	$2.27 \pm 0.1$	$0.81 \pm 0.05$
3	850	28	$2.17 \pm 0.1$	$4.60 \pm 0.1$
		32	$2.06 \pm 0.1$	$3.14 \pm 0.1$
		36	$1.50 \pm 0.1$	$0.87 \pm 0.05$
		40	$1.65 \pm 0.1$	$0.85 \pm 0.05$
		44	$1.92 \pm 0.1$	$0.80 \pm 0.05$
		48	$2.21 \pm 0.1$	$0.78 \pm 0.05$

tural changes zone was made on the etched cross-sections. The effects of remelting were evaluated based on macro- and microscopic examinations, X-ray structural studies, and hardness measurement. The microstructure tests were carried out using an Olympus GX41 light microscope and a JOEL JSM-6610LV scanning electron microscope. The specimens for microstructural investigations were polished and etched to reveal the grain boundary. A fracture for fractographic research was obtained by breaking a sample using Charpy hammer. The sample was previously cut on the side opposite the modified surface, and the cut depth was about 5 mm. The macroscopic analysis was carried out using an Olympus SZ61 stereoscopic microscope. X-ray phase composition tests were carried out using a Seifert XRD-3003 X-ray diffractometer, with cobalt lamp radiation  $\lambda_{\text{CoK}\alpha 1} = 0.17902$  nm. The angular step was  $0.05^\circ$  and the pulse counting time was 6 s. The hardness was measured using a Shimadzu HVM-G20 microhardness tester equipped with a Vickers penetrator. A load of 1961.4 mN and a load time of 10 s were used.

### 3. Results and discussion

**3.1. Macroscopic investigations.** An important aspect of the work was to assess the possibilities of shaping the dimensions of the zone of microstructural changes by appropriate selection of treatment parameters. Analysis of the nature and size of the changes in the material microstructure as a function of the laser processing parameters showed several relationships. Namely, it was found that by reducing  $\Delta l$ , i.e. the distance of the irradiated surface from the focus of the beam focusing system, an increase in the depth of structural changes is obtained in all samples, but only in some samples there is a simultaneous reduction in the bandwidth (in this case the bandwidth is understood as the remelting diameter in the place of laser beam interaction). In the case of bands obtained at the smallest  $\Delta l$  values, i.e. equal to 28 and 32 mm, the bands had a very irregular and variable shape, as a result of which the remelting width varied depending on the place of measurement and no rational relationship was found in this case. This condition should be explained by an extremely dynamic course of the remelting process as well as the crystallization of the material itself, which was accompanied by the least favorable changes in the geometric structure of the surface of all the remelted samples. During the research it was found that the bandwidth and remelting depth decrease with increasing the speed of the laser head. Apart from the bands obtained at  $\Delta l = 28$  mm and 32 mm, the largest remelting width of approximately 2.32 mm was obtained after applying  $\Delta l = 48$  mm and  $V = 750$  mm/min, and the smallest width of approximately 1.50 mm in the case of the remelted band using  $\Delta l = 36$  mm and  $V = 850$  mm/min. On the other hand, the largest penetration depth of approximately 1.07 mm was obtained for the sample melted using  $\Delta l = 36$  mm and  $V = 750$  mm/min, and the smallest penetration depth of approximately 0.78 mm was obtained after using  $\Delta l = 48$  mm and  $V = 850$  mm/min. The width and depth of the bands were measured on transverse metallographic specimens. Extremely high heating and

cooling speeds occurring during remelting increase the risk of cohesion loss in the solidifying material. This risk in the case of a material produced by powder metallurgy may be increased by the pores present in the material, which may cause uneven heat flow from the remelting zone. Therefore, when assessing machining efficiency, particular attention was paid to the presence of this type of structural defects in the laser beam interaction zone.

Microcracks were found only in the case of the remelted samples using  $\Delta l = 28$  mm and  $\Delta l = 32$  mm and, as can be seen in Fig. 1, in most cases they were on the edge of the band or slightly touched the remelting zone. For the remaining samples, no cracks, discontinuities, or porosity were found. Examples of the macroscopic effects of the remelting samples are shown in Fig. 1. Figure 2 shows cross sections of the laser-treated bands. The width and depth of the microstructural changes were measured.

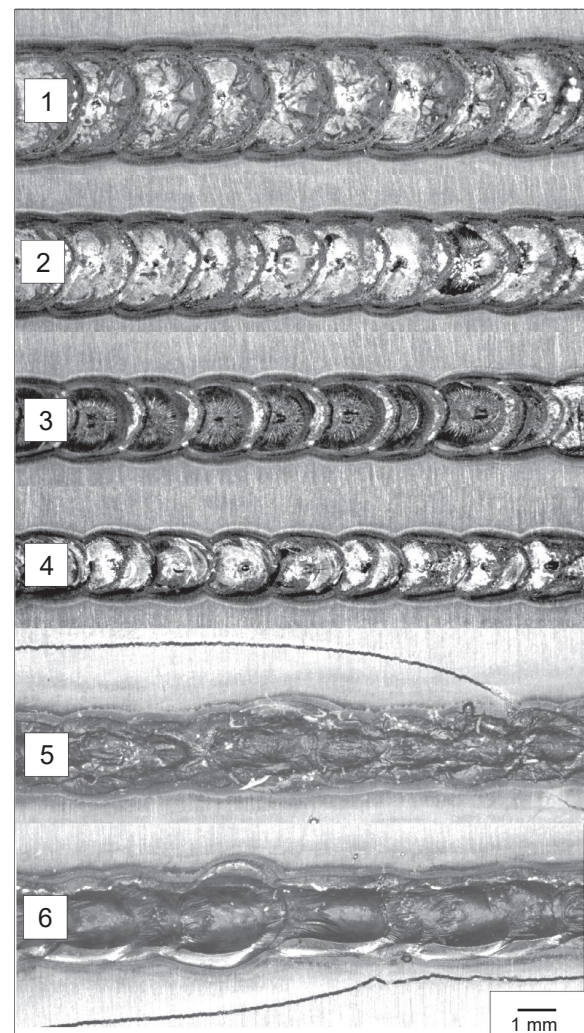


Fig. 1. Example macroscopic effects of sample remelting. Face of bands. Laser processing parameters: 1)  $V = 800$  mm/min and  $\Delta l = 48$  mm; 2)  $V = 800$  mm/min and  $\Delta l = 44$  mm; 3)  $V = 800$  mm/min and  $\Delta l = 40$  mm; 4)  $V = 800$  mm/min and  $\Delta l = 36$  mm; 5)  $V = 800$  mm/min and  $\Delta l = 32$  mm; 6)  $V = 800$  mm/min and  $\Delta l = 28$  mm

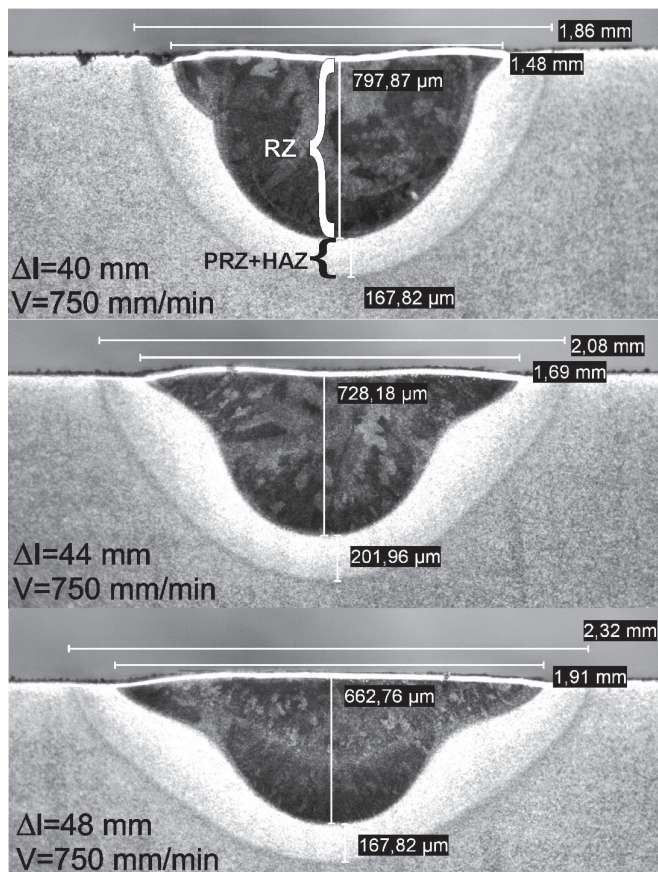


Fig. 2. Etched cross-sections of melted bands

**3.2. Microstructural investigations.** The microstructure of high-speed steel in its initial state is shown in Fig. 3. The carbides were evenly distributed within the matrix and their diameter was less than 2 μm. There was no carbide banding in the material or uneven concentration of carbides in the sample volume. Such effects are often observed in high-speed steels manufactured in a conventional manner. The steel was characterized by high homogeneity in the distribution of carbides and a homogeneous chemical composition. The lack of segregation and homogeneity of the microstructure prove the isotropic nature of powder steel.

The microstructure of laser-remelted P/M HSS is shown in Figs. 4 and 5. As a result of remelting treatment, characteristic zones were formed in the surface layer, i.e. a distinctly dominant remelting zone (RZ) and the following: a partial remelting zone (PRZ) and a heat affected zone (HAZ) adjacent to the core material (BM). Similar facts were reported in [19]. The presence of distinct microdendritic structures was found in the full remelting zone (Figs. 5a, b and c). Microdendrites occurred in the entire volume of the remelting zone and were characterized by a compact structure and a very small distance between the secondary axes. The average distance between the secondary axes of dendrites was below 1 μm (Fig. 5a), which proves very high material cooling rates. A characteristic feature of the microstructure in the RZ was the dissolution of primary carbides, and the presence of extremely fine, network-like car-

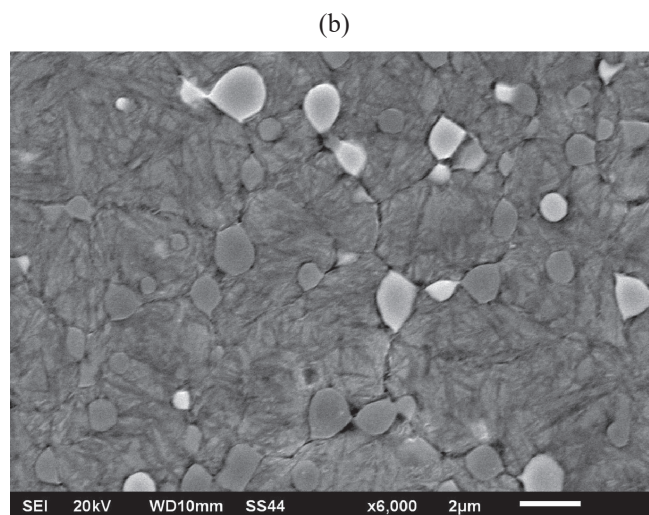
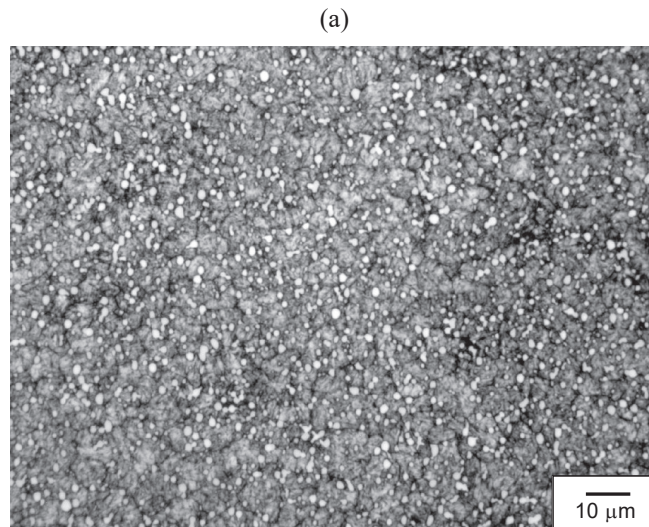
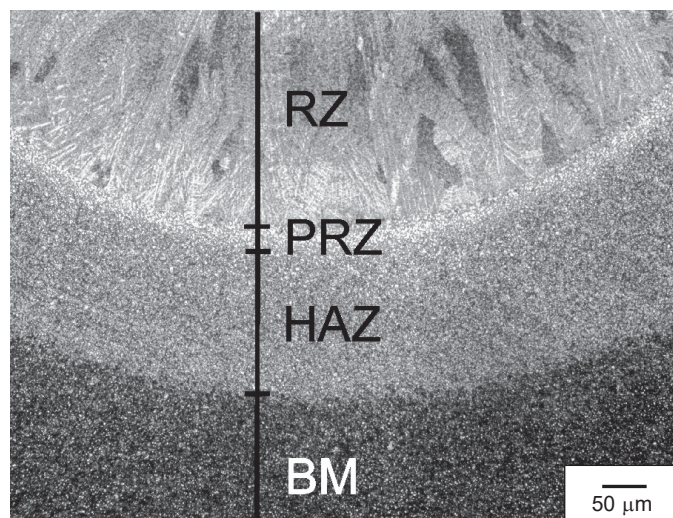


Fig. 3. Etched microstructure of P/M HSS. Light microscopy (a), SEM (b)

Fig. 4. Etched microstructure of melted band.  $V = 750$  mm/min,  $\Delta l = 48$  mm

## Laser surface remelting of powder metallurgy high-speed steel

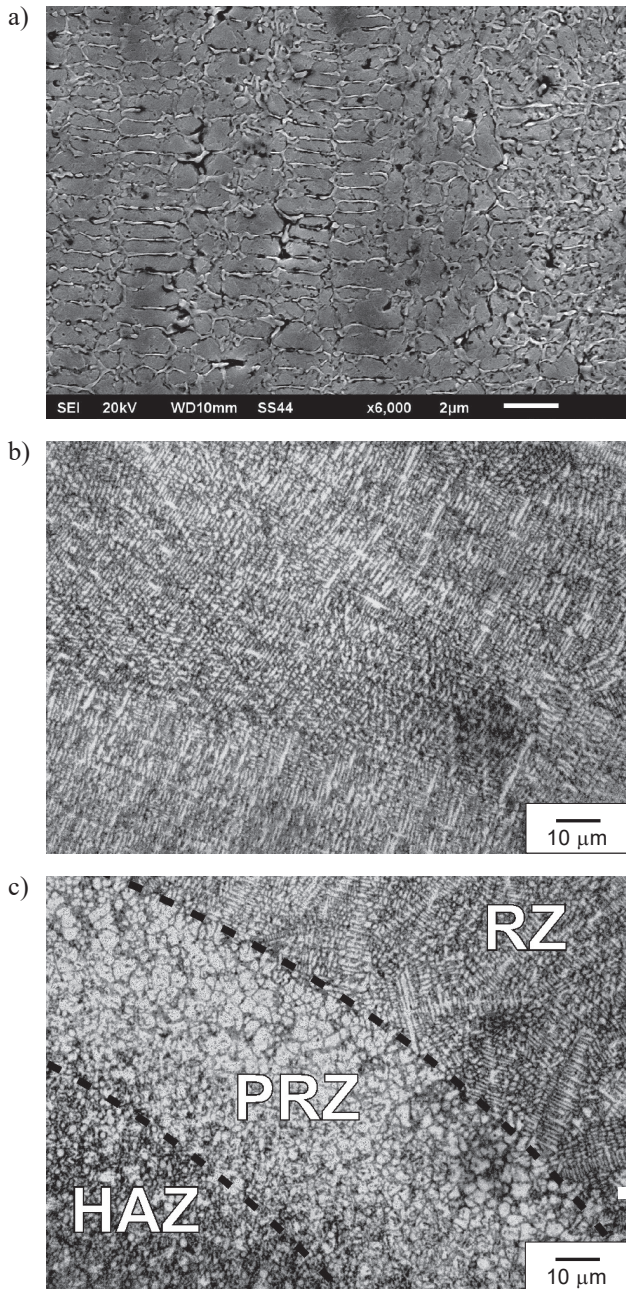


Fig. 5. Etched microstructure in RZ (a, b), in RZ, PRZ and HAZ (c). SEM (a), light microscopy (b, c).  $V = 750$  mm/min,  $\Delta l = 48$  mm

bide precipitates in the interdendritic spaces. The morphology of these carbides was different from the morphology of the primary carbides observed in the starting material. The presence of network carbide precipitates in laser surface melted high speed steel was observed by Chau et al. [14], among others. Between the RZ and the HAZ a narrow heterogeneous partially remelted zone was observed (Figs. 4 and 5c). The thickness of PRZ was from  $\sim 20$  to  $60$   $\mu\text{m}$ , depending on the laser processing parameters used. The microstructure of PRZ consisted of extremely fine equiaxed grains with a diameter of  $1$  to  $5$   $\mu\text{m}$  and a partial dissolution of primary carbides. Equiaxed grains dominated especially near the border with the RZ. The num-

ber of carbides in PRZ was lower than in the core, but as the core approached, the content of undissolved carbides distinctly increased.

The border between the full remelting zone and the partial remelting zone was very clear as opposed to the border between the PRZ and HAZ. In this case, there was a smooth transition from the partial remelting zone to the heat affected zone. In the wide heat affected zone, the temperature was not high enough to melt the steel and only solid-state phase transformations occurred.

The microscopic studies were enriched with fractography. The nature of material fracture constitutes one of the criteria of the initial quality assessment of the material, its homogeneity and purity, susceptibility to cracking/breaking, mechanical properties, etc. Examination of the initial steel revealed distinct isotropicity of the material and the presence of residual porosity. Completely different effects were found in the material subjected to laser treatment. A distinct microdendritic microstructure was found in the remelting zone. A characteristic effect was also the orientation of the crystallization products, reflecting the direction of heat outflow from the remelting zone. The material structure was very compact, and the residual porosity was practically eliminated, the assessment was based in this case on SEM investigations. Similar facts were reported by [2]. The fracture of the P/M HSS sample in its initial state is shown in Fig. 6a, while after remelting with a laser in Fig. 6b.

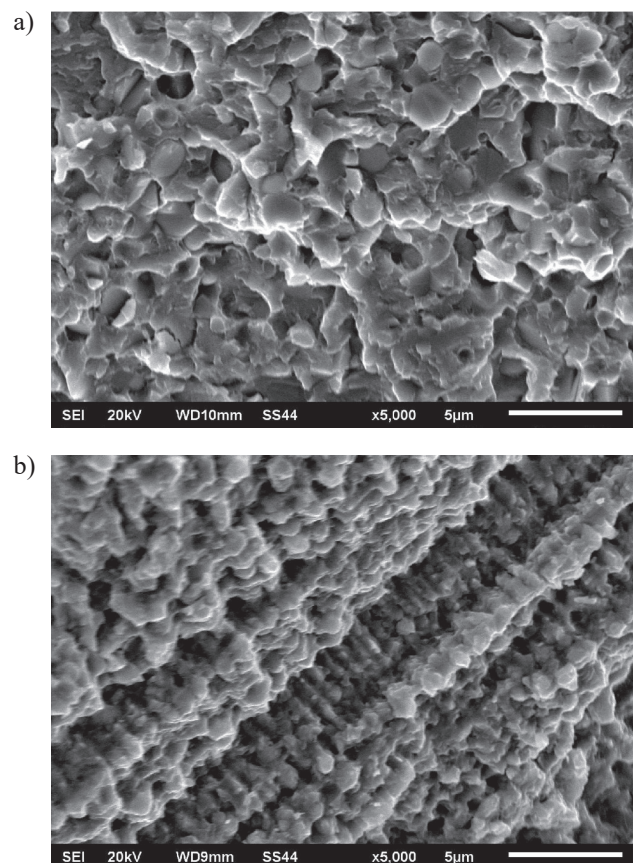


Fig. 6. Fracture in non-remelted part (a), in remelted part (b)

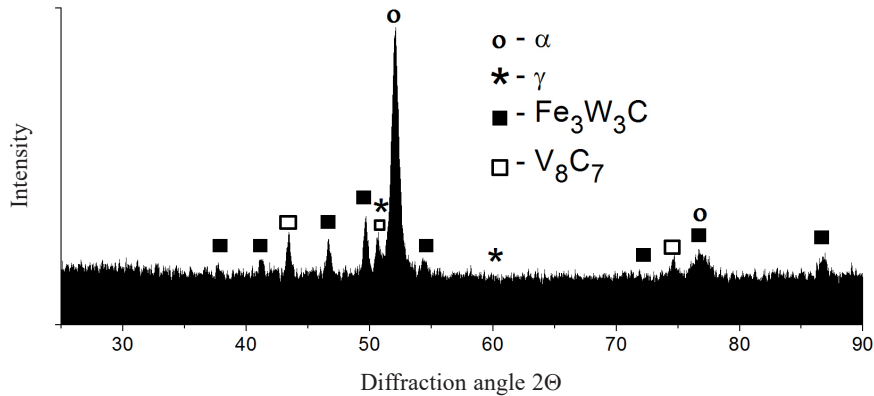


Fig. 7. Diffractogram of non-remelted P/M HSS

**3.3. XRD investigations.** In its initial state, i.e. after quenching and tempering, the analyzed steel had a tempered martensite structure with fine and evenly distributed carbides,  $M_6C$  ( $V_8C_7$ ) and  $M_6C$  ( $Fe_3W_3C$ ) types, and a low content of retained austenite. The retained austenite content was about 9%, as determined by X-ray diffraction. An example X-ray diffractogram of the starting material (non-remelted) is shown in Fig. 7. In the case of the remelted material, the surface of the bands was subjected to X-ray analysis. Prior to X-ray examinations, the surface of the bands was subjected to grinding with 600 grit sandpaper to eliminate surface irregularities that could affect the accuracy of the analysis. Phase composition studies revealed the presence of retained austenite, martensite, and carbide phases in the remelted material. A reduction in the intensity of diffraction reflections from the carbide phases was found in relation to the starting material, which can be explained by the complete dissolution of primary carbides in the steel matrix during laser processing and the pre-

cipitation of less numerous extremely fine, network-like carbide in the interdendritic spaces. The laser processing parameters affect not only the scope of microstructural changes, but also the type of these changes, as the cooling rate of the material changes. As is well known, the value of the  $M_s$  (Martensite start) and  $M_f$  (Martensite finish) points decrease as the cooling rate increases. A high cooling rate can therefore depress martensitic transformation and increase the content of retained austenite [16, 27].

During the research, a relationship was found between the content of retained austenite in individual samples and heat source speed  $V$ , and lack of a distinct relationship between the content of retained austenite and the value of parameter  $\Delta l$ . A sample remelted using  $\Delta l = 36$  mm at variable speeds  $V = 750$  mm/min, 800 mm/min and 850 mm/min was analyzed as well as a remelted sample using  $\Delta l = 48$  mm, 44 mm, 40 mm and 36 mm at constant speed  $V = 750$  mm/min. The test results are shown in Fig. 8. As can be seen, the content of

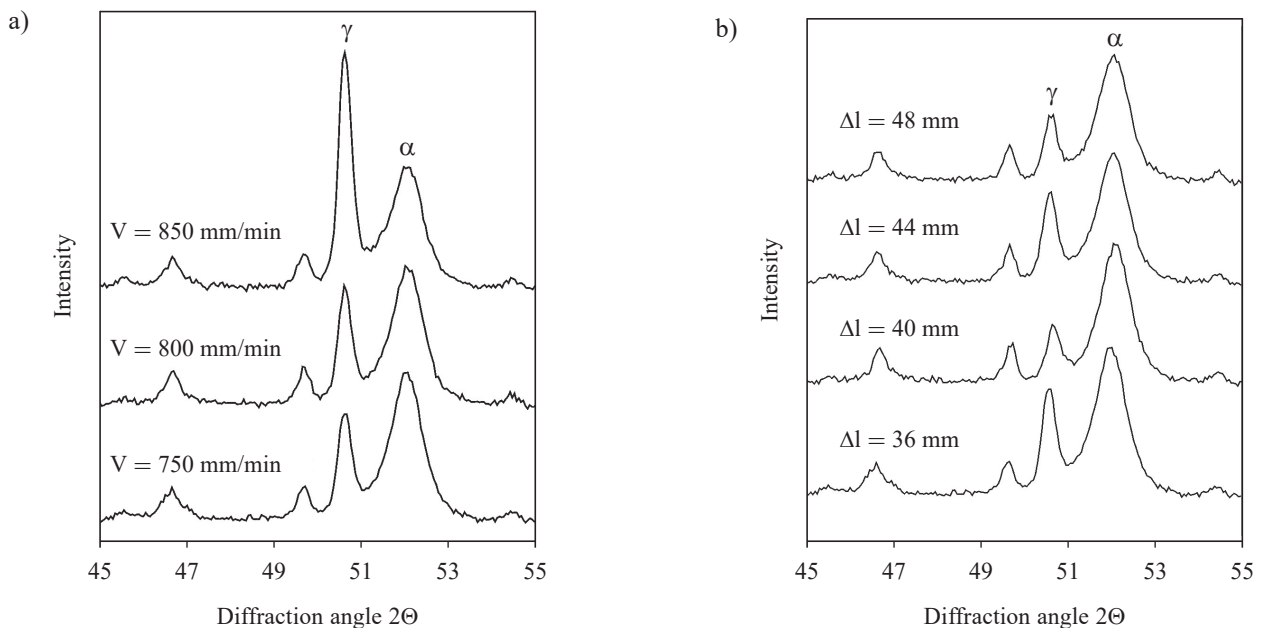


Fig. 8. Change in content of retained austenite depending on laser beam speed  $V$  at constant value of  $\Delta l = 36$  mm (a); change in content of retained austenite depending on value of parameter  $\Delta l$  at constant speed  $V = 750$  mm/min

retained austenite increased with an increase in the laser beam speed  $V$  and at  $V = 850$  mm/min retained austenite became the dominant phase in the steel. However, it can also be seen that the increase in austenite content was not proportional to the increase in the value of parameter  $V$ . At  $V = 750$  mm/min and 800 mm/min, the differences in the content of retained austenite were much smaller compared to the content of retained austenite recorded in the sample remelted at  $V = 850$  mm/min. The impact of the parameter  $\Delta l$  value on the content of retained austenite was no longer so unambiguous and described by a simple relationship. The retained austenite content increased with an increase in the  $\Delta l$  value; however, at  $\Delta l = 40$  mm a lower retained austenite content than in the other samples was observed.

**3.4. Hardness results.** The correlation between the applied remelting treatment parameters and hardness of P/M HSS was analyzed. The hardness measurements were made only for bands in which no disqualifying macroscopic changes were noted, which means that the bands obtained at  $\Delta l = 28$  mm and  $\Delta l = 32$  mm were not subjected to hardness measurements.

The analyzed samples showed a decrease in hardness in all the bands compared to the hardness of the material without treatment. The decrease in hardness was mainly caused by the presence of retained austenite in the microstructure of the remelted material. The changes in the hardness as a function of the distance from the remelted surface are presented in Fig. 9. The average hardness of the material in the full remelting zone was about 780 HV0.2, and in the heat affected zone about 870 HV0.2. The average hardness of the non-remelted material was about 960 HV0.2. Therefore, it was higher by about 23% than the hardness in the remelting zone and by about 10% higher than the average hardness of the material in the heat affected zone. A decrease in the hardness of high-speed steel after surface remelting was also found by other authors analyzing the effect of surface remelting on the microstructure and surface properties of high-speed steels [14]. In the case of

the heat affected zone, a large scatter of hardness values was also found, greater than in the full remelting zone. The analysis of hardness variability as a function of the machining parameters did not show distinct regularities between the obtained hardness and the values of the  $\Delta l$  or  $V$  parameters. The decrease in hardness of the remelted layer should be explained by both the presence of retained austenite and the complete dissolution of primary carbides in the steel matrix. However, it should be noted that despite such a significant content of retained austenite, the observed decrease in hardness is relatively small, which can be explained by a small grain size, precipitation of ultra-fine dispersed carbides and high solute content. According to Jurci et al. [21], the final hardness of the remelted steel is a result of the competition between the extension of solid solutions and high portion of retained austenite. In this case, an extremely high retained austenite volume fraction is the dominant factor leading to a decrease in hardness.

## 4. Summary

The aim of this work was to study the changes in the structure, microstructure, and hardness of P/M high-speed steel remelted by a laser beam. It was found that CO<sub>2</sub> laser treatment leads to significant changes in the microstructure of the surface layer of steel, whose nature and scope result from the very rapid heating of the material as well as its rapid cooling and crystallization. As a result of laser processing, a full remelting zone is formed in the surface layer of the steel, characterized by a compact microdendritic structure and the presence of extremely fine, network-like carbide precipitates in the interdendritic spaces. The primary carbide particles were completely dissolved during laser remelting treatment. The orientation of the main axes of the microdendrites corresponded to the direction of heat transfer. The remelting zone was a distinctly dominant zone in relation to the other zones formed as a result of surface treatment, i.e. the partially remelted zone and the non-remelted heat affected zone. The effects of remelting treatment, and especially the dimensions of the remelting zone, can be controlled by appropriate association of the basic treatment parameters, i.e. focus distance from the sample surface and the laser head speed. The depth of microstructural changes decreases with an increased distance of the irradiated surface from the focus of the focusing system or with an increased speed of the laser head. In turn, the remelting bandwidth decreases with a decrease in  $\Delta l$ , i.e. the distance of the irradiated surface from the focus of the beam focusing system, and to a limited extent also with an increase in the heat source speed. The width of the remelted surface layer obtained after laser treatment varied from 1.50 mm to 2.32 mm, and the depth varied from 0.78 mm to 1.07 mm. Remelting treatment facilitates the elimination of residual porosity of powder steels, which can contribute to the increased toughness and cutting performance of steel. The microstructure of the laser remelted steel consists of martensite, retained austenite and carbides. The retained austenite content increases with increasing  $V$ , while the influence of the  $\Delta l$  parameter on the retained austenite content is not unequiv-

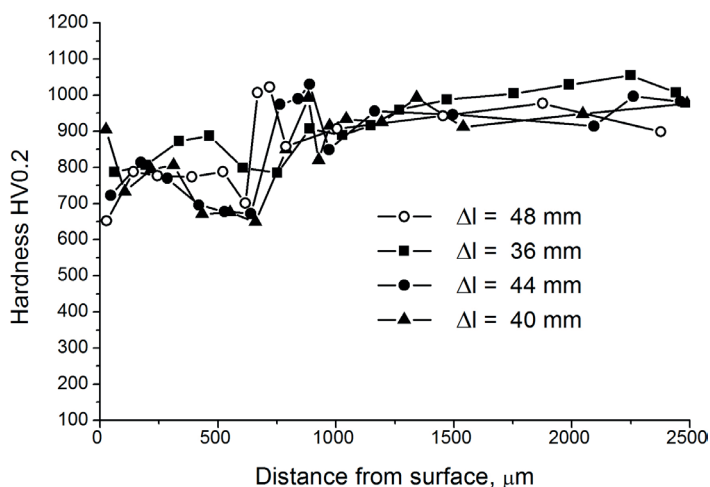


Fig. 9. Distribution of hardness as a function of distance from surface, sample No. 1 ( $V = 750$  mm/min)

ocal. Due to the high content of retained austenite in the remelted layer and the dissolution of primary carbides in the steel matrix, the hardness of high-speed steel after remelting is unfortunately reduced, which should be taken into account at the stage of choosing the method of processing these steels.

## REFERENCES

- [1] W. Shen, L. Yu, H. Liu, Y. He, Z. Zhou, and Q. Zhang, "Diffusion welding of powder metallurgy high speed steel by spark plasma sintering", *J. Mater. Process. Technol.* 275, 116383 (2020).
- [2] R. Colaco, E. Gordo, E.M. Ruiz-Navas, M. Otasevic, and R. Vilar, "A comparative study of the wear behaviour of sintered and laser surface melted AISI M42 high speed steel diluted with iron", *Wear* 260, 949–956 (2006).
- [3] N. Chen, R. Luo, H. Xiong, and Z. Li, "Dense M2 high speed steel containing core-shell MC carbonitrides using high-energy ball milled M2/VN composite powders", *Mater. Sci. Eng. A* 771, 138628 (2020).
- [4] G. Zhang, H. Yuan, D. Jiao, Z. Li, Y. Zhang, and Z. Liu, "Microstructure evolution and mechanical properties of T15 high speed steel prepared by twin-atomiser spray forming and thermo-mechanical processing", *Mater. Sci. Eng. A* 558, 566–571 (2012).
- [5] H. Peng, L. Hu, L. Li, L. Zhang, and X. Zhang, "Evolution of the microstructure and mechanical properties of powder metallurgical high-speed steel S390 after heat treatment", *J. Alloys. Compd.* 740, 766e773 (2018).
- [6] J. Kusinski *et al.*, "Laser modification of the materials surface layer – a review paper", *Bull. Pol. Ac.: Tech.* 60(4), 711–728 (2012).
- [7] Y. Li, S. Arthanari, and Y. Guan, "Influence of laser surface melting on the properties of MB26 and AZ80 magnesium alloys", *Surf. Coat. Technol.* 378, 124964 (2019).
- [8] J. Iwaszko and K. Kudła, "Surface modification of ZrO<sub>2</sub>–10 wt.% CaO plasma sprayed coating", *Bull. Pol. Ac.: Tech.* 64(4), 937–942 (2016).
- [9] M. Szafarska, J. Iwaszko, K. Kudła, and I. Łęgowik, "Utilisation of high-energy heat sources in magnesium alloy surface layer treatment", *Arch. Metall. Mater.* 58(2), 619–624 (2013).
- [10] J. Iwaszko and M. Strzelecka, "Effect of cw-CO<sub>2</sub> laser surface treatment on structure and properties of AZ91 magnesium alloy", *Opt. Laser. Eng.* 81, 63–69 (2016).
- [11] J. Winczek, A. Modrzycka, and E. Gawrońska, "Analytical description of the temperature field induced by laser heat source with any trajectory", *Procedia Eng.* 149, 553–558 (2016).
- [12] G. Gontarz, T. Chmielewski, and D. Golański, "Modification of sprayed aluminum layers on steel substrate by the concentrated heat source", *Weld. Tech. Rev.* 83(12), 52–55 (2011).
- [13] C.T. Kwok, F.T. Cheng, and H.C. Man, "Microstructure and corrosion behavior of laser surface-melted high-speed steels", *Surf. Coat. Technol.* 202(2), 336–348 (2007).
- [14] A.S. Chaus, A.V. Maksimenko, N.N. Fedosenko, E. Čaplovič and V.N. Myshkovets, "Formation of structure of a high-speed steel upon laser surface melting", *Phys. Met. Metallogr.* 120(3), 269–277 (2019).
- [15] R. Ulewicz and F. Nový, "Influence of laser treatment on properties of high speed tool", *Tech. Trans.* 10, 195–200 (2018).
- [16] K.Y. Benyounis, O.M. Fakron, and J.H. Abboud, "Rapid solidification of M2 high-speed steel by laser melting", *Mater. Design* 30, 674–678 (2009).
- [17] S. Kac, J. Kusinski, A. Zielinska-Lipiec, and I. Wrońska, "Scanning electron microscopy and transmission electron microscopy microstructural investigation of high-speed tool steel after Nd:YAG pulsed laser melting", *J. Microsc.* 224, 65–67 (2006).
- [18] S. Kac and J. Kusinski, "SEM and TEM microstructural investigation of high-speed tool steel after laser melting", *Mater. Chem. Phys.* 81(2), 510–512 (2003).
- [19] J. Arias, M. Cabeza, G. Castro, I. Feijoo, P. Merino, and G. Pena, "Microstructural characterization of laser surface melted AISIM2 tool steel", *J. Microsc.* 239, 184–193 (2010).
- [20] J. Arias, M. Cabeza, G. Castro, I. Feijoo, P. Merino, and G. Pena, "Modification of AISI M2 high-speed tool steels after laser-surface melting under different operating conditions", *Weld. Int.* 27, 1–9 (2013).
- [21] P. Jurči, J. Cejp, and J. Brajer, "Metallurgical aspects of laser surface processing of PM Cr-V ledeburitic steel", *Adv. Mater. Sci. Eng.* 563410 (2011).
- [22] A. Surzhenkov, G. Allikas, A. Gregor, S. Zimakov, P. Kulu, and H. Müller, "Laser treatment of surfaces of tool and PM steels and steels with coatings", in *6th International DAAAM Baltic Conference Industrial Engineering*, 2008.
- [23] R. Vilar, R. Colaço, and A. Almeida, "Laser surface treatment of tool steels", *Opt. Quant. Electron.* 27(12), 1273–1289 (1995).
- [24] W. Bochnowski, "The influence of arc plasma electric and laser treatment on the structure and properties of the high speed steel", *Arch. Foundry Eng.* 9(3), 17–20 (2009).
- [25] C.T. Kwok, F.T. Cheng, H.C. Man, and K.I. Leong, "Laser surface melting of high-speed steels for enhancing surface properties", in *Conference: ICALEO®. 24th International Congress on Laser Materials Processing and Laser Microfabrication*, 2005.
- [26] W. Bochnowski, H. Leitner, L. Major, R. Ebner, and B. Major, "Primary and secondary carbides in high-speed steels after conventional heat treatment and laser modification", *Mater. Chem. Phys.* 81(2–3), 503–506 (2003).
- [27] Y. Luo, H. Guo, X. Sun, M. Mao, and J. Guo, "Effects of austenitizing conditions on the microstructure of AISI M42 high-speed steel", *Metals* 7, 27 (2017).